

Colloidal Stability of Gold Nanoparticles Coated with Multithiol-Poly(ethylene glycol) Ligands: Importance of Structural Constraints of the Sulfur Anchoring Groups

Eunkeu Oh, Kimihiro Susumu, Antti Johannes Makinen,
Jeffrey R. Deschamps, Alan L. Huston, and Igor L. Medintz

J. Phys. Chem. C, **Just Accepted Manuscript** • DOI: 10.1021/jp405265u • Publication Date (Web): 13 Aug 2013

Downloaded from <http://pubs.acs.org> on August 19, 2013

Just Accepted

“Just Accepted” manuscripts have been peer-reviewed and accepted for publication. They are posted online prior to technical editing, formatting for publication and author proofing. The American Chemical Society provides “Just Accepted” as a free service to the research community to expedite the dissemination of scientific material as soon as possible after acceptance. “Just Accepted” manuscripts appear in full in PDF format accompanied by an HTML abstract. “Just Accepted” manuscripts have been fully peer reviewed, but should not be considered the official version of record. They are accessible to all readers and citable by the Digital Object Identifier (DOI®). “Just Accepted” is an optional service offered to authors. Therefore, the “Just Accepted” Web site may not include all articles that will be published in the journal. After a manuscript is technically edited and formatted, it will be removed from the “Just Accepted” Web site and published as an ASAP article. Note that technical editing may introduce minor changes to the manuscript text and/or graphics which could affect content, and all legal disclaimers and ethical guidelines that apply to the journal pertain. ACS cannot be held responsible for errors or consequences arising from the use of information contained in these “Just Accepted” manuscripts.



Report Documentation Page

Form Approved
OMB No. 0704-0188

Public reporting burden for the collection of information is estimated to average 1 hour per response, including the time for reviewing instructions, searching existing data sources, gathering and maintaining the data needed, and completing and reviewing the collection of information. Send comments regarding this burden estimate or any other aspect of this collection of information, including suggestions for reducing this burden, to Washington Headquarters Services, Directorate for Information Operations and Reports, 1215 Jefferson Davis Highway, Suite 1204, Arlington VA 22202-4302. Respondents should be aware that notwithstanding any other provision of law, no person shall be subject to a penalty for failing to comply with a collection of information if it does not display a currently valid OMB control number.

1. REPORT DATE 13 AUG 2013	2. REPORT TYPE	3. DATES COVERED 00-00-2013 to 00-00-2013			
4. TITLE AND SUBTITLE Colloidal Stability of Gold Nanoparticles Coated with Multithiol-Poly(ethylene glycol) Ligands: Importance of Structural Constraints of the Sulfur Anchoring Groups		5a. CONTRACT NUMBER			
		5b. GRANT NUMBER			
		5c. PROGRAM ELEMENT NUMBER			
6. AUTHOR(S)		5d. PROJECT NUMBER			
		5e. TASK NUMBER			
		5f. WORK UNIT NUMBER			
7. PERFORMING ORGANIZATION NAME(S) AND ADDRESS(ES) U.S. Naval Research Laboratory, Optical Sciences Division, Code 5611, Washington, DC, 20375		8. PERFORMING ORGANIZATION REPORT NUMBER			
9. SPONSORING/MONITORING AGENCY NAME(S) AND ADDRESS(ES)		10. SPONSOR/MONITOR'S ACRONYM(S)			
		11. SPONSOR/MONITOR'S REPORT NUMBER(S)			
12. DISTRIBUTION/AVAILABILITY STATEMENT Approved for public release; distribution unlimited					
13. SUPPLEMENTARY NOTES J. Phys. Chem. C, 13 Aug 2013					
14. ABSTRACT					
15. SUBJECT TERMS					
16. SECURITY CLASSIFICATION OF:			17. LIMITATION OF ABSTRACT Same as Report (SAR)	18. NUMBER OF PAGES 32	19a. NAME OF RESPONSIBLE PERSON
a. REPORT unclassified	b. ABSTRACT unclassified	c. THIS PAGE unclassified			

1
2
3
4
5
6
7
8
9 **Colloidal Stability of Gold Nanoparticles Coated with Multithiol-**
10 **Poly(ethylene glycol) Ligands: Importance of Structural Constraints**
11 **of the Sulfur Anchoring Groups**
12

13
14
15 **Eunkeu Oh,* Kimihiro Susumu, Antti J. Mäkinen, Jeffrey R. Deschamps, Alan L. Huston**
16 **and Igor L. Medintz***
17

18
19
20 Dr. A. J. Mäkinen, Dr. A. L. Huston
21 U.S. Naval Research Laboratory
22 Optical Sciences Division, Code 5611
23 Washington, DC 20375 USA

24
25 Dr. J.R. Deschamps, Dr. I. L. Medintz
26 U.S. Naval Research Laboratory
27 Center for Bio/Molecular Science and Engineering, Code 6900
28 Washington, DC 20375 USA

29
30 Dr. E. Oh, Dr. K. Susumu
31 Sotera Defense Solutions
32 Annapolis Junction, MD 20701 USA

33
34 E-mail: eunkeuoh@ccs.nrl.navy.mil (Tel: 202-404-2519);
35 igor.medintz@nrl.navy.mil (Tel: 202-404-6046)
36
37
38
39
40
41
42
43
44
45
46
47
48
49
50
51
52
53
54

Abstract

Gold nanoparticles (AuNPs) coated with a series of poly(ethylene glycol) (PEG) ligands appended with four different sulfur-based terminal anchoring groups (monothiol, flexible dithiol, constrained dithiol, disulfide) were prepared to explore how the structures of the sulfur-based anchoring groups affect the colloidal stability in aqueous media. The PEG-coated AuNPs were prepared by ligand exchange of citrate-stabilized AuNPs with each ligand. The colloidal stability of the AuNPs in different harsh environmental conditions was monitored visually and spectroscopically. The AuNPs coated with dithiol- or disulfide-PEG exhibited improved stability under high salt concentration and against ligand replacement competition with dithiothreitol compared with those coated with their monothiol counterpart. Importantly, the ligands with structurally constrained dithiol or disulfide showed better colloidal stability and higher sulfur coverage on the Au surface compared to the ligands with more flexible dithiol and monothiol. X-ray photoelectron spectroscopy also revealed that the disulfide-PEG ligand had the highest Au-S ratio on the Au surface among the ligands studied. This result was supported by energy minimization modeling studies: the structurally more constrained disulfide ligand has the shortest S-S distance, and could pack more densely on the Au surface. The experimental results indicate that the colloidal stability of the AuNPs is systematically enhanced in the following order: monothiol < flexible dithiol < constrained dithiol < disulfide. The present study indicates that the colloidal stability of thiolated ligand-functionalized AuNPs can be enhanced by (i) a multidentate chelating effect and (ii) use of the constrained and compact structure of the multidentate anchoring groups.

Keywords: Disulfide, Bidentate, Monothiol, Constrained dithiol, DTT

1. Introduction

The application of colloidal inorganic nanoparticles (NPs) in biology has grown tremendously in the past decade, and this has been driven primarily by the ever increasing range of their utility.¹⁻¹³ As perhaps the most common NP material, gold NPs (AuNPs) are now found in various biologically-related roles including signal transducers in colorimetric assays and diagnostics, energy transfer quenchers, cellular labels, multi-photon imaging, single molecule tracking and delivery vehicles along with platforms for photothermal therapy.^{1, 2, 6-8, 14-18} For effective performance within most biological applications, colloidal AuNPs are required to be biocompatible and highly stable in biological environments. More specifically, they need to fulfill the following expectations: (1) high solubility in aqueous environments; (2) resistance towards ionic molecules (e.g., NaCl, NaOH, HCl) found in biological buffers; (3) resistance to reducing agents such as dithiothreitol (DTT), tris(2-carboxyethyl)phosphine (TCEP), mercaptoethanol, glutathione and cysteine; and (4) low nonspecific binding to the abundant biomolecules in biological serum (e.g., proteins, peptides, nucleic acids); (5) resistance to heat treatments (e.g., >80 °C for DNA hybridization).^{6-8, 16, 17, 19} As AuNPs are not colloiddally stable in solvent or aqueous environments without surfactants, almost all AuNPs are stabilized or modified with surface ligands or other functionally-related (bio)molecules which promote their dispersion, prevent aggregation and sometimes provide additional chemical groups or 'handles' for further bioconjugation.^{1, 3, 5-7} Thus, the colloidal stability of AuNPs is directly affected by the physical and chemical properties of the ligands, and the design of ligands is critically important to the overall experimental results in biological applications.

Most surface ligands are modular in nature and typically consist of an anchoring group for attachment to the AuNP surface, a backbone or spacing group, and a terminal functional group(s); the latter often display different chemical groups to impart various properties to the AuNP such as charge and a reactive site.^{2, 3, 16, 20} Interaction between anchoring groups and the AuNP surface can be driven by different types of mechanisms such as metal-ligand coordination (S-Au bonding, carboxyl-Au interaction, histidine-Au coordination), electrostatic attraction (positively charged peptide/protein/polymer - negatively charged AuNP) and hydrophobic adsorption (hydrophobic protein pockets - AuNP).^{1, 20} Each mechanism will also be characterized by different affinities and avidities. The chain length and hydrophobicity of the ligand backbone can also affect the

1
2
3
4
5
6
7
8
9 quality of the ligand layer surrounding the AuNPs as well as the overall solubility. For example,
10 an alkyl chain backbone contrasts well with a poly(ethylene glycol) (PEG) backbone in this
11 matter. The nature of the terminal functional groups can be modified to control repulsive or
12 attractive forces between the AuNPs and other molecules for nonfouling or electrostatic
13 conjugation properties, respectively. Alternatively, the termini can be designed to display groups
14 for specific conjugation chemistries such as carbodiimide coupling (amine-carboxyl group), click
15 chemistry (alkyne-azide) and biomolecular interaction (biotin-avidin, glycan/carbohydrates-
16 lectins).^{3, 16}

17
18
19
20
21 A wide variety of surface ligands have been developed to modify the surface and improve
22 the colloidal characteristics of AuNPs.^{1, 19, 21-45} Citric acid has been the most commonly used
23 ligand when negatively charged surfaces or a rather loose ligand shell is required for further
24 modification.²¹ Phosphine or phosphine oxide derivatives were used for preparation of smaller
25 sized AuNPs (1.5 nm diameter).²² Cetyltrimethylammonium bromide (CTAB) has been
26 frequently used as a cationic surfactant.²³ Amine-stabilized AuNPs have also been prepared
27 using octadecylamine / tri-*n*-octylphosphine oxide (TOPO),²⁴ oleylamine²⁵ and L-lysine.²⁶
28 Pyridine and similar molecules have also been applied for modification of AuNPs.²⁷ AuNP
29 colloidal stability has been significantly improved by preparing a relatively thicker shell with
30 polymers or polyelectrolytes such as poly(N-vinyl-2-pyrrolidone) (PVP),²⁹ polyethylenimine
31 (PEI),³⁰ thioether-terminated polymers,³¹ poly(*p*-phenyleneethynylene),³² silica,³³ and
32 multidentate polymers.³⁴ Since Brust's report of a synthetic method using dodecanethiol to
33 make strong coordinating bonds with Au, thiol-based ligands have now become one of the most
34 popular ligands for stabilizing AuNPs due to the strong Au-S binding.³⁵ Colloidal stability of
35 AuNPs for biological applications has been demonstrated by a variety of thiol-based ligands such
36 as mercaptopropionic acid,³⁶ glutathione,³⁷ thiol-terminated poly(ethylene glycol) (PEG-SH),^{19,}
37 ^{38,39} dithiocarbamate,²⁸ a multidentate-PEG,^{40-42, 46, 47} a multidentate-zwitterionic ligand,⁴⁷ thiol-
38 terminated DNA,⁴³ cysteine-containing peptides⁴⁴ and bovine serum albumin (BSA).⁴⁵ On the
39 other hand, the structural changes of thiol anchoring groups have been tried to enhance the
40 stability of AuNPs. Shulz et al studied the effect of the spacer structure on the stability of
41 AuNPs with PEG-SH.¹⁹ Mirkin et al. studied the importance of multidentate structures of thiol
42 anchoring groups attached to DNA to enhance the stability of DNA-coated AuNPs.⁴³ To the
43 contrary, Hou et al. reported that the cyanide etching and oxidation rates of dithiolate-stabilized
44
45
46
47
48
49
50
51
52
53

1
2
3
4
5
6
7
8
9 small AuNPs (1-3 nm) was faster than those of the dodecanethiolate- or mixed ligand-stabilized
10 AuNPs.⁴⁸ Our group demonstrated that the coordination number of the ligands attached to the
11 AuNPs played an important role in colloidal stability. Dithiol-PEG ligand has been shown to
12 enhance the stability of AuNPs and quantum dots (QDs) compared to monothiol-PEG ligands.⁴¹
13 ⁴⁹ Dithiol-PEG-stabilized AuNPs showed long-term stability across a wide range of pHs (pH 2-
14 13) and in high salt concentration (2M NaCl) due to the high water solubility of PEG and the
15 strong binding of dithiol to the NP surfaces. We have also found that small AuNPs with high
16 curvature are more sensitive to cyanide etching and need ligands capable of a high surface
17 packing density to improve the colloidal stability.^{41, 49} The previous study indicated that balance
18 between the coordination number and surface packing density of the ligands is crucial to enhance
19 the colloidal stability of AuNPs.
20
21
22
23
24

25 In the present study, we investigated how the structural differences of sulfur-based bidentate
26 anchoring groups affect the colloidal stability of AuNPs. The focus of this study is on the
27 spacing between the sulfur anchoring groups in the ligand, structural constraints and flexibility of
28 the anchoring groups as well as the distance between the backbone and the sulfur anchoring
29 group. For this, we designed four different ligands with different sulfur-based anchoring groups,
30 and prepared AuNPs coated with those ligands (AuNP-PEGs). While each ligand (MP7M,
31 BP7M, DP7M and TP7M) has an identical PEG backbone (averaged molecular weight ~ 750
32 Da) and a methoxy terminal group, each of them has a different sulfur-based anchoring group,
33 see Figure 1a. MP7M has a monothiol originated from mercaptohexanoic acid. BP7M has a
34 dithiol anchoring group with a relatively flexible structure and spacing between the two thiol
35 units. DP7M has a dithiol anchoring group originated from dihydrolipoic acid (DHLA). TP7M
36 has a disulfide anchoring group from thioctic acid (TA, closed-ring form of DHLA). MP7M has
37 one thiol for each PEG chain, and the others have two thiols (or one disulfide) for each PEG
38 chain. The influence of the different anchoring group on the colloidal stability of the aqueous
39 phase AuNP-PEGs was explored side by side under the following conditions: (a) high salt
40 concentrations (2M NaCl), (b) in the presence of dithiothreitol (DTT), which has strong binding
41 affinity with Au surfaces and could replace the original ligands, and (c) at high temperature. Our
42 present study demonstrated that the bidentate ligands (dithiol and disulfide) and in particular, the
43 structurally constrained disulfide anchoring group enhanced the NPs' tolerance to high ionic
44
45
46
47
48
49
50
51
52
53
54

1
2
3
4
5
6
7
8
9 buffer conditions, high temperatures, and competition against the other strong Au binding
10 reagents.

11
12 The degree of thiol coverage on the Au surface for each ligand was studied using X-ray
13 photoelectron spectroscopy (XPS). The following relationships were established: (i) the sulfur-
14 based bidentate PEGs exhibited a higher Au-S binding ratio (higher S coverage) than the
15 monothiol-PEG; (ii) AuNPs assembled with the bidentate ligands were more colloiddally stable
16 than the monothiol-PEG AuNPs, despite the smaller number of PEG units per thiol (one PEG
17 ligand per bidentate thiol ligand (1 PEG, 2 S), compared to one PEG ligand per monothiol
18 ligand(1 PEG, 1 S) (iii) the more structurally constrained the two sulfur atoms (the bidentate
19 ligands) were, the higher S coverage on the surface of Au. We also estimated the distances
20 between two sulfur atoms in the bidentate-PEGs based on energy minimization, and compared
21 the stable anchoring positions of two adjacent sulfurs of each ligand on the Au surface. This
22 modeling suggests that a match between the sulfur atom separation within the ligand and the
23 distance of adjacent Au atoms on the AuNP surface is critical for a good thiol coverage on the
24 NP surface and overall colloidal stability.
25
26
27
28
29
30
31
32
33

34 2. Experimental Section

35 2.1. Synthesis of ligands: MP7M, DP7M, TP7M, BP7M

36 All of the PEG ligands studied here were synthesized from methoxy-terminated PEG (MeO-
37 PEG750-NH₂) with an average molecular weight of ~750 (ethylene oxide repeat units n ~15).
38 Methoxy-terminated PEG-modified monothiol ligand (MP7M), PEG-modified thioctic acid
39 ligand (TP7M) or PEG-modified dihydrolipoic acid ligand (DP7M) were synthesized, and
40 characterized following the procedures detailed in the references.^{41, 50} See Figure 1 for the
41 relevant structures of ligands. PEG-modified dithiol ligand with relatively flexible structure
42 (BP7M) was synthesized by procedures detailed in the Supporting Information.
43
44
45
46
47
48

49 2.2. Preparation of AuNPs

1
2
3
4
5
6
7
8
9 We prepared AuNP-PEG using 15 nm sized citrate-stabilized AuNPs (Ted Pella, Inc.) by ligand
10 exchange method.⁴⁰ Each ligand was added to the citrate-stabilized AuNP dispersion in water at
11 pH 8-8.5 (adjusted from deionized water using NaOH) and stirred for 8 hours. 10 ml of AuNPs
12 stock solution (2.3 nM) was mixed with 26 μmol of the bidentate ligand (BP7M, DP7M, or
13 TP7M) or 51 μmol of the monodentate ligand (MP7M). The total ratio of thiol-to-Au surface
14 atoms in the reaction mixture was ~ 200 . After stirring the reaction mixture at room temperature
15 overnight, free ligands were removed by three cycles of concentration/dilution using a membrane
16 filtration device (Millipore, 100 KDa molecular weight cut-off). Deionized water was used for
17 purifying the AuNP dispersion. Each AuNP dispersion displaying the different ligands was then
18 concentrated up to 4 - 5 times ($\sim 10 - 11$ nM) in water and stored at 4 $^{\circ}\text{C}$ until use.

23 2.3. XPS analysis

24
25
26 Self-assembled monolayers (SAMs) of each ligand were deposited by dipping flame-annealed
27 Au substrates into the dipping solution. Flame annealing produces Au films with predominantly
28 (111) surfaces.⁵¹ The concentration of the dipping solution containing each ligand was fixed to
29 130 mM for the bidentate ligands (BP7M, DP7M, TP7M) and 260 mM for the monodentate
30 ligands (MP7M and mercaptoundecanoic acid (MUA)) in water. MUA-SAM was used as control.
31 A cleaned, flame-annealed Au substrate was immersed into each solution overnight and washed
32 with methanol and water three times. The Au-SAM surface was dried and kept under N_2 for
33 further use. XPS analysis was performed using a Thermo Scientific K-Alpha XPS
34 instrumentation with a monochromatic Al K-Alpha source, and the spectral peaks of core levels
35 were fitted using commercial XPS analysis software. The fitted functional form was a single
36 Voigt doublet superimposed on a Shirley-type (Au) or polynomial (S) background function.⁵²

42 2.4. Molecular modeling of ligands and ligand-gold interactions

43
44
45 All models were created using tools in UCSF Chimera (version 1.4.1). Energy minimization was
46 carried out in Chimera using the built-in features including ANTECHAMBER (version 1.27) and
47 the AM1-BCC method of calculating charges.⁵³ The gold surface was created using the cubic
48 form of gold with $a = b = c = 4.0786$ \AA and the Fm3m space group. Based on Au-S interactions
49 found in the Cambridge Structural Database (CSD) (www.ccdc.cam.ac.uk/products/csd/), the
50 Au-S bond distance was set to be 2.3 \AA when docking ligands onto the Au surface.
51
52

3. Results and Discussion

3.1. Synthesis of ligands and AuNPs

Four sulfur-based ligands were synthesized from MeO-PEG750-NH₂⁵⁰ by amide bond formation with different sulfur anchoring groups (Figure 1a): (1) monothiol-PEG (MP7M) with mercaptohexanoic acid,⁴¹ (2) dithiol-PEG (BP7M) with cystamine derivatives (Figure S1, Supporting Information), (3) dithiol-PEG (DP7M) with dihydrolipoic acid (DHLLA), (4) disulfide-PEG (TP7M) with thioctic acid (TA).⁵⁰ Each synthesized ligand has the same methoxy-terminated PEG with different structures within the sulfur-based anchoring groups. This allows us to examine how the structural differences of the sulfur-based anchoring groups affect the colloidal stability of AuNPs. The AuNPs coated with each ligand (AuNP-PEGs: AuNP-MP7M, AuNP-BP7M, AuNP-DP7M, AuNP-TP7M) were prepared by ligand exchange from commercial citrate-stabilized AuNPs (Ted Pella, Inc., diameter ~15 nm).⁴¹ We used excess amounts of the ligands (ratio of thiol-to-Au surface atom ~ 200) in slightly basic pH (8-8.5); this condition enhances the Au-S interaction and helps the ligands effectively replace the original citrate ligands of AuNPs. Previously we confirmed the effectiveness of our ligand exchange protocol by comparing the FT-IR spectra collected from TP7M-modified AuNPs and free ligand (TP7M), compared to citrate AuNPs. The amide bonding (C=O stretch at ~1670 cm⁻¹/ N-H bending at ~1540 cm⁻¹) and CH₂ vibrational mode (~2850, ~2920 cm⁻¹) of AuNP-TP7M matched well those of TP7M, and there was no distinguishable contribution from citrates (original large C=O stretch band at ~1590 cm⁻¹ of citrate is gone).⁴⁹ The absorption spectra of AuNP-PEGs showed no significant change from that of the original citrate-stabilized AuNPs (AuNP-Citrate) (Figure 1b); there was neither apparent shift of the surface plasmon resonance band (SPB) at 520 nm nor absorbance changes over a wide wavelength range. While the hydrodynamic size in intensity mode measured by dynamic light scattering slightly increased after ligand exchange due to the length of PEG, the data showed no apparent sign of aggregation (Figure 1c and Table S1 in supporting information). The main peak was observed around 23~24 nm in the intensity profile of DLS, indicating no aggregation after ligand exchange over time except AuNP-MP7M showing very small tail. This result indicates that AuNP-PEGs have no microscopic aggregations

1
2
3
4
5
6
7
8
9 and surface etching after ligand exchange. The TEM images also showed no specific aggregation
10 or size change in all the AuNP-PEGs samples after ligand exchange (data not shown).⁴⁹ Thus,
11 PEG modification of AuNP surfaces was successfully carried out, and the sample preparation
12 process was consistent for all the ligands.
13

14 15 3.2. Colloidal stability tests: high ionic solution, reducing reagent and aggregation factor 16

17
18 Using as-prepared AuNP-PEGs with different ligands, we examined the long-term colloidal
19 stability under harsh environmental conditions. First, we tested the resistance of AuNP-PEGs in
20 a high ionic buffer (2 M NaCl in water). Ionic buffers or salt solutions are commonly used in
21 biological studies and frequently cause NP aggregation due to (i) screening repulsive forces
22 between NPs originating from the surface ligands and (ii) decreased solubility of the ligands.⁵⁴
23 Since most of the AuNP-PEGs studied here were found to be very stable even in high salt
24 concentration at room temperature,⁴¹ we sped up the aging process of AuNP-PEGs by heating
25 the dispersion at 100 °C in 2M NaCl solutions. Because of no colloidal color differences
26 between four AuNP-PEGs samples (with different ligands) and the same absorption spectra
27 before adding NaCl (Figure 1b), we chose freshly prepared AuNP-TP7M as the control sample
28 (marked as Cont. in the first column of Figure 2). After 5 minutes of heating, AuNP-MP7M
29 dramatically changed to grey due to fast aggregation, and AuNP-BP7M turned purple (Figure 2a).
30 The color of the AuNP-DP7M changed to light pink in 5 minutes and almost transparent in 15
31 minutes, presumably due to aggregation or adsorption onto the vial surface. However, the AuNP-
32 TP7M colloidal solution turned to a darker purple color than three other samples after 15
33 minutes of heating in 2M NaCl, which indicated slower or less aggregation. To monitor microscopic
34 changes of AuNP-PEGs under this high ionic condition, we also measured the absorption spectra
35 (Figure 3). The absorption spectra of AuNP-MP7M and AuNP-BP7M became broader and the
36 peak position of surface plasmon resonance band (SPB) was shifted bathochromically, which
37 reflects the aggregation of AuNPs. The absorbance of the AuNP-DP7M solution decreased
38 significantly while the AuNP-TP7M solution showed a relatively smaller decrease. For
39 quantitative comparison of microscopic changes of AuNP-PEGs, we defined the accumulated
40 flocculation (*AF*) as the increase of accumulated absorbance from 600 nm to 900 nm per
41 absorbance at 520 nm (the peak of the original SPB):
42
43
44
45
46
47
48
49
50
51

$$AF = I/A - I_0/A_0 \quad (1)$$

where I_0 and I are total area from 600 to 900 nm in the absorption spectra of AuNP-PEGs before and after 15 minutes of heating in 2M NaCl, respectively (Figure 5a). A_0 and A are the absorbance at 520 nm before and after 15 minutes of heating in 2M NaCl, respectively. The higher AF value simply reflects the higher degree of aggregation. Monothiol-modified AuNP (AuNP-MP7M) showed the most accumulated flocculation after heating ($AF = 191$), and dithiol-modified AuNPs (AuNP-BP7M and AuNP-DP7M) showed less aggregation ($AF = 60 \sim 63$), which is $\sim 30\%$ of AuNP-MP7M (Figure 5b). Disulfide-modified AuNP (AuNP-TP7M) showed the least aggregation ($AF = 36$) which is $\sim 20\%$ of monothiol-modified AuNP and $\sim 60\%$ of the dithiol-modified AuNPs. This result indicates that the NP aggregation in high salt buffer is sensitive to the number of anchoring groups as well as their structures, and the close geometry of two sulfur atoms of the anchoring groups may be beneficial to effectively prevent NP aggregation.

Next, we examined the resistance of AuNP-PEGs in the presence of the strong reducing agent, dithiothreitol (DTT). DTT is commonly used to reduce disulfide bonds in a variety of biomolecules including peptides, proteins, antibodies, and thiol-modified DNAs.¹⁶ At high concentration, DTT can effectively displace the original ligands on the NP surface and bind to the AuNP surface because of its dithiol group and compact structure, which eventually leads to NP aggregation.^{40, 41, 55, 56} Therefore, strong resistance in the presence of DTT is particularly promising for applying AuNPs within biological assays, which are often carried out in media containing small thiol molecules such as cysteine, glutathione, mercaptoethanol, and DTT. We monitored the spectral changes of AuNP-PEGs in the presence of 1.5 M DTT, 0.8 M NaCl and 10 mM NaOH; basic pH buffer makes DTT more reactive. The DTT concentration used here is much higher than those measured for thiol-containing molecules in biological environments; for example, intracellular glutathione level is estimated to be 1 \sim 10 mM.⁵⁷ While the monothiol-modified AuNP (AuNP-MP7M) immediately showed precipitation and completely lost the original red colloidal color in less than 20 minutes, while the other dithiol-modified AuNPs (AuNP-BP7M and AuNP-DP7M) were relatively stable for 20 minutes and the disulfide-modified AuNP (AuNP-TP7M) showed very little change even after 90 minutes (Figure 2b). The time variation of the absorption spectra of AuNP-PEGs showed microscopic changes of

1
2
3
4
5
6
7
8
9 each sample from 0 to 20 minutes after adding DTT solution (Figure 4). Overall, the spectral
10 changes were similar to those of the NaCl test. The peak of SPB was bathochromically shifted
11 due to aggregation of AuNPs and formation of their large clusters. The intensity of SPB also
12 decreased due to precipitation of AuNPs. The absorption spectra of AuNP-MP7M changed
13 faster than those of the other three AuNP-PEGs. The corresponding progression of accumulated
14 flocculation, AF , with time was plotted in Figure 5c. AuNP-MP7M showed the most significant
15 aggregation and the AF steeply increased in the first 10 minutes and was gradually saturated (AF
16 ~ 120). AuNP-BP7M and AuNP-DP7M had relatively smaller AF values (40 \sim 50) than AuNP-
17 MP7M, and AuNP-TP7M showed the smallest AF values (~ 30) which is $\sim 25\%$ of monothiol-
18 modified AuNP and $\sim 60\%$ of the dithiol-modified AuNPs. This trend of AF differences in DTT
19 test was very similar to that noted in the previous NaCl test. The SPB shifts also dramatically
20 increased with time (Figure 5d). The monothiol ligand (AuNP-MP7M) and relatively flexible
21 dithiol ligand (AuNP-BP7M) resulted in large bathochromic SPB shifts (130 \sim 160 nm in 20
22 minutes), indicating NP aggregation. On the other hand, the structurally constrained dithiol
23 (AuNP-DP7M) and disulfide (AuNP-TP7M) ligands led to a smaller SPB shift (60 \sim 70 nm in 20
24 minutes) and slower aggregation of AuNPs. These side-by-side comparisons observed for mono-,
25 dithiol- and disulfide-modified AuNPs suggest that the dominant factor for stabilizing AuNPs
26 against surface invasion by small thiolated molecules (DTT) is not only the multidentate nature
27 of the anchoring groups but also the structural constraint at the anchoring units (in DP7M and
28 TP7M), which modulate the overall ligand binding strength onto the metal surface. Enhanced
29 stability of metal (Au, Ag) NPs using thioctic acid modified oligonucleotides in the presence of
30 10 mM DTT has been previously reported.⁵⁶

3.3. Surface coverage of ligands: XPS analysis

31
32
33
34
35
36
37
38
39
40
41
42
43 For further investigation of the binding properties affected by the different ligand structures, X-
44 ray photoelectron spectroscopy (XPS) was used to analyze bonding of the sulfur-based anchoring
45 groups onto the Au surface. SAMs of the ligands were prepared on the Au surface by dipping
46 the Au substrates into each ligand solution. Core level shifts in the XPS spectra are indicative of
47 the chemical state of the emitting atom, and intensities of the emitted photoelectrons can be used
48 for quantitative analysis of the chemical compositions. Additionally, the intensities of
49 photoelectrons of the monolayers coated by four different PEG ligands can be used to estimate
50
51
52
53
54

the relative surface coverage of the adsorbed species. In the plot of intensity vs. binding energy (158 ~ 168 eV) (Figure 6a), only S 2p doublets (S 2p_{3/2,1/2}) were observed around 162.1 and 163.2 eV for the monothiol-modified Au surface (Au-MP7M) and the disulfide-modified Au surface (Au-TP7M). This result indicates that only the bound sulfur species are present on the Au surface, and a single layer of sulfur atoms is formed at the Au-S interface as expected for a well-formed SAM. In the case of dithiol-modified Au surface (Au-DP7M, Au-BP7M), there were small intensity contributions from unbound species of S 2p_{3/2,1/2} around 163.4 and 164.6 eV, overlapping partially in energy with the bound species and giving rise to triple peak feature in the raw data. The surface coverage of S atoms was calculated using S 2p (bound) and Au 4f (substrate) intensities. Because Au 4f, and S 2p photoelectron intensities are nearly identically attenuated by the hydrocarbon overlayer (due to their similar kinetic energies), a simple ratio of S/Au photoelectron intensities can be used to obtain the absolute sulfur coverage (n_s):^{58, 59}

$$n_s = \left(\frac{I_S}{I_{Au}} \frac{\sigma_{Au}}{\sigma_S} \right) \left(\frac{T_{Au}}{T_S} L_{Au}^0 N_{Au} \right) \quad (2)$$

where I_S and I_{Au} are the measured photoelectron intensities, and σ_S and σ_{Au} are photoelectron cross sections for the S 2p and Au 4f core levels, respectively. T_{Au}/T_S is the energy analyzer transmission function, N_{Au} is the bulk atomic density of Au substrate ($5.892 \times 10^{22} \text{ cm}^{-3}$), and L_{Au}^0 is the electron attenuation length for quantitative analysis (1.745 nm) obtained from reference 48. While the sulfur coverage of the monothiol-PEG (MP7M) derived monolayer was calculated to be 4.4×10^{14} of sulfur atoms/cm², those of dithiol-PEGs were 5.8×10^{14} and 5.2×10^{14} atoms/cm² for BP7M and DP7M, respectively (Table 1). In contrast to the monothiol-PEG or dithiol-PEGs, n_s of the disulfide-PEG derived monolayer (6.8×10^{14} sulfur atoms/cm²) was even higher. The SAM of MUA was also prepared as control and its coverage was 6.7×10^{14} atoms/cm². The sulfur coverage in our experiment was higher than that in a previous report, in which the sulfur coverage for a complete alkanethiol on Au estimated by experiment and theory was $5.0 \times 10^{14} \text{ cm}^{-2}$ and $4.6 \times 10^{14} \text{ cm}^{-2}$, respectively.⁶⁰ This comparison suggests that the thiol-coverage obtained from our experiment could be slightly an overestimate. Nevertheless, the relative thiol-coverage is still valid for comparison purpose. First, when we consider the number of sulfur atoms per ligand, the monothiol-PEG (MP7M) is expected to have the largest number

of “PEG” ligands on the Au surface ($4.4 \times 10^{14} / \text{cm}^2$) because of the 1:1 ratio of PEG:S for the monothiol-PEG and 1:2 ratio of PEG:S for the dithiol or disulfide-PEG ($2.6 \sim 3.4 \times 10^{14} / \text{cm}^2$). Even with the larger number of PEG ligands on the Au surface, the monothiol-PEG showed weaker colloidal stability in the previous NaCl and DTT tests because only one thiol anchoring group keeps the PEG ligand from dissociating from the Au surface. Second, considering the structural differences between bidentate PEG, two sulfur atoms of the disulfide unit in TP7M could have a higher chance to bind closely together than two sulfur atoms of less structurally constrained dithiols in BP7M and DP7M. A similar result was reported in the spectroscopic study of Au-S bond formation in monolayers derived from a dithiol monomer and related disulfide-containing polyamides.⁶¹ In that report, the disulfide-containing polymer was attached to the Au surface through both sulfur atoms of the monomer unit to form the anticipated surface-attached loop. In contrast, the dithiol monomer was adsorbed mostly through a single thiol end; another thiol end was unbound. The XPS results can be correlated with the colloidal stability (as determined using NaCl and DTT tests) in two important points; (i) the strong binding of multidentate ligand to the NPs contributed to colloidal stability more dominantly than the total PEG ligand number on NPs, (ii) the structural constraint of two sulfur atoms of the bidentate ligands led to better sulfur atom coverage on the NP surface, which directly reflected the higher colloidal stability.

3.4. Molecular modeling of ligand structures and ligand-gold interactions

To better understand the interactions between the sulfur atoms and the gold surface, we modeled the distances between sulfur atoms in dithiol-PEG (BP7M, DP7M) and disulfide-PEG (TP7M) using UCSF Chimera (version 1.4.1).⁵³ A summary of the S-S and Au-Au distances for each ligand was given in Table 2 and the relative conformations of each anchoring group on the Au surface were pictured in Figure 6b. For this, we chose the lowest energy conformer presenting a geometric compatible with both sulfur atoms of each ligand interacting with a flat gold surface. If the lowest energy conformer did not fit this condition, the other low energy conformers were examined and reported in the Table 2. The simulated distance of two sulfur atoms in each single ligand (S-S distance) was 5.84 Å for BP7M and 4.35 (R isomer) - 4.92 (S isomer) Å of DP7M. In the case of disulfide-PEG in TP7M, the S-S distance was 2.03 Å, which is the shortest among the bidentate ligands studied here. This means that TP7M has more of a structural constraint in

1
2
3
4
5
6
7
8
9 its anchoring group than the two other bidentate ligands, DP7M and BP7M. In order to simplify
10 the further analysis, the structures of DHLA and TA without PEG were also examined, see
11 Figure S2 and S3. In the case of DHLA and TA, the S-S distance in each ligand was 4.22 (*R*
12 isomer) - 4.92 (*S* isomer) and 2.02 Å, respectively, which shows a trend similar to the structures
13 of the same anchoring groups with PEGs, DP7M and TP7M. The positions of the protons
14 attached to the sulfur atoms were changed to place the lone pairs in a position where the
15 interaction with the Au surface was likely to be maximized. This rotation is not required for TA,
16 but the positions of the lone pairs are fixed such that an optimal interaction may require a tilt of
17 the whole molecule relative to the surface. The possible low energy conformers of these two
18 ligands are shown in Figure S4, and their relative positions on Au surface are pictured in Figure
19 7a. Within all the sulfur-based bidentate ligands, the Au-S interaction is most likely preferred on
20 a pair of gold atoms (Au-Au) separated by either 4.08 Å or 2.88 Å (Table 2, blue circles and red
21 circles in Figure 7b, respectively). In the case of dithiol in DHLA, cleavage of the sulfur-sulfur
22 bond results in structural relaxation, which easily accommodates the Au-Au distance, either two
23 threefold hollow sites (the empty sites in the center between three neighboring Au atoms, Figure
24 7b, Blue filled circles) or two bridge sites (the middle sites between two neighboring Au atoms,
25 Figure 7b, Blue open circles) on hexagonal close packed Au fcc (111) surface.^{17, 62} In the case of
26 the disulfide in TA, we can suggest an optimal fit when the two S head groups occupy
27 asymmetric bonding sites on the Au surface, with one S located approximately in the Au hollow
28 site and the other S located near the adjacent Au bridge site (Figure 7b, Red filled circles)
29 because the S-S bond distance of TA (2.02 Å) does not match the distance between the hollow
30 sites of Au(111) (1.7 or 2.9 Å).^{62, 63} This free-ligand modeling simply demonstrates that the
31 constrained disulfide ligand (TA or TP7M) could have a greater chance to pack more densely on
32 the Au surface than the flexible dithiol ligands because of the closer S-S distance compared to
33 the other ligands. The modeling studies discussed here are consistent with the experimental
34 results. The structurally constrained disulfide ligand showed the higher sulfur coverage on Au
35 surface and higher colloidal stability on the AuNPs than the flexible dithiol ligands despite the
36 fact that the Au surface and AuNP have different curvature and slightly different Au lattice
37 structure.
38
39
40
41
42
43
44
45
46
47
48
49
50
51
52
53
54
55
56
57
58
59
60

1
2
3
4
5
6
7
8
9
10
11
12
13
14
15
16
17
18
19
20
21
22
23
24
25
26
27
28
29
30
31
32
33
34
35
36
37
38
39
40
41
42
43
44
45
46
47
48
49
50
51
52
53
54
55
56
57
58
59
60

Conclusion

Here, we studied how the structures of anchoring groups of surface ligands affect the colloidal stability of AuNPs using a series of PEG-based modular ligands appended with four different sulfur-based anchoring groups (monothiol, flexible dithiol, constrained dithiol and disulfide). The PEG-coated AuNPs were prepared by ligand exchange of citrate-stabilized AuNPs with each ligand. The colloidal stability of the AuNPs in harsh environmental conditions was monitored visually and spectroscopically. The AuNPs coated with dithiol- or disulfide-PEG exhibited much better stability under high salt concentration (2M NaCl at 100 °C) and against ligand replacement competition with DTT (1.5 M) than those coated with their monodentate counterpart. Furthermore, XPS analysis revealed that the disulfide-PEG ligand had the highest Au-S ratio on the Au surface, indicating the highest surface coverage among them. This implies the ligands with structurally constrained dithiol or disulfide showed better colloidal stability and higher sulfur coverage on the Au surface compared to the ligands with more flexible dithiol and monothiol. The XPS data were also supported by structural modeling studies of the ligands: structurally constrained disulfide ligand showed the smallest S-S distance and such a compact bidentate structure could have a higher chance of dense packing on the Au surface. The present study indicates that the colloidal stability of NPs can be significantly enhanced by (i) a multidentate chelating effect and (ii) use of a constrained and compact structure within the anchoring groups. These aspects would certainly help us design more sophisticated surface ligand structures and enhance the colloidal stability of NPs, which is a crucial parameter for a variety of biological applications.

Acknowledgements. This work was supported by NRL, ONR, DARPA, and DTRA. We thank Dr. Fredrik K. Fatemi for useful discussions about the results.

Supporting Information Available. The synthesis of ligand, hydrodynamic size of AuNP-ligands, molecular modeling were included in the supporting information. This information is available free of charge via the Internet at <http://pubs.acs.org>.

Table 1. Relative sulfur coverage of each ligand on Au surface analyzed by XPS. The surface coverage of S atoms was calculated using S 2p and Au 4f (substrate) intensities as described.

	MP7M	BP7M	DP7M	TP7M
Sulfur Coverage ($\times 10^{14}$ atoms/cm ²)	4.4 \pm 0.16	5.8 \pm 0.30	5.2 \pm 0.56	6.8 \pm 0.85

Table 2. Distances (Å) in gold-sulfur complexes for each ligand.

Compound	S-Au	S-S	Au-Au ^c
MP7M	2.29	NA	NA
BP7M	2.35, 2.30	5.84 \pm 1.35 ^a	4.08
DP7M	2.35, 2.31	4.35 (<i>R</i>), 4.92 (<i>S</i>) ^b	4.08
TP7M	2.45, 2.30	2.03	2.88
DHLA	2.32, 2.29	4.22 (<i>R</i>), 4.92 (<i>S</i>) ^b	4.08
TA	2.27, 2.27	2.02	2.88

^a The average value of multiple conformations in the case of BP7M is presented here, because there are primarily two dihedrals having two minima giving multiple conformations are within a few kcal.

^b *R* and *S* indicate the enantiomers of DP7M and DHLA since DHLA (dihydrolipoic acid or 6,8-dimercaptooctanoic acid) has a chiral center at C6 position. Those two enantiomers have slightly different low energy conformer for both sulfur atoms interacting with a flat gold surface.

^c The corresponding Au-Au separation with each ligand docking on the Au surface in the energy minimization model (Blue circles and Red circles, respectively in Figure 7b)

Figure Caption

Figure 1. (a) Chemical structures of the series of PEG ligands with different sulfur-based anchoring groups: MP7M, BP7M, DP7M, TP7M. (b) The absorption spectra of AuNPs before (AuNP-citrate) and after ligand exchange with the PEG ligands: AuNP-MP7M (Red), AuNP-BP7M (Orange), AuNP-DP7M (Green) and AuNP-TP7M (Blue). (c) Dynamic light scattering (DLS) data of AuNPs before (AuNP-citrate) and after ligand exchange with the PEG ligands: AuNP-MP7M (Red), AuNP-BP7M (Orange), AuNP-DP7M (Green) and AuNP-TP7M (Blue) were the data of 2 year-old sample after ligand exchange. AuNP-TP7M (Blue dotted line) is measured just after ligand exchange as a fresh sample control.

Figure 2. Side-by-side comparisons of the dispersion stability of AuNPs with different ligands (marked at the bottom of pictures as MP7M, BP7M, DP7M and TP7M). The images of freshly prepared AuNP-TP7M (Control) were also shown in parallel to see the sample color changes during the experiments. (a) NaCl and heat resistance test: colloidal AuNPs in 2M NaCl after 0, 5 and 15 minutes at 100 °C (the first three pictures). Heat resistance test: colloidal AuNPs after heating (100 °C) in 2M NaCl during 15 minutes followed by 24 hours at room temperature (the last picture). (b) DTT resistance test: colloidal AuNPs in 1.5 M DTT, 0.8 M NaCl and 10 mM NaOH after 1, 4, 20, 60 and 90 minutes at room temperature.

Figure 3. UV-vis absorption spectra of 15 nm AuNP dispersions before (solid line) and after (dotted line) heating in 2 M NaCl aqueous solution for 15 min: (a) MP7M-AuNPs; (b) BP7M-AuNPs; (c) DP7M-AuNPs; (d) TP7M-AuNPs.

Figure 4. Time course measurements of the UV-vis absorption spectra of 15 nm AuNP dispersions with 1.5 M DTT, 0.8 M NaCl and 10 mM NaOH in water: (a) MP7M-AuNPs; (b) BP7M-AuNPs; (c) DP7M-AuNPs; (d) TP7M-AuNPs in 0.2, 0.3, 0.5, 1, 2, 3 minutes, and every 2 minutes from 4 to 20 minutes; the surface plasmon bands shift from left to right.

Figure 5. (a) The concept of the accumulated flocculation of AuNP-PEGs using UV-vis absorption spectrum based on equation (1). (b) The accumulated flocculation (AF) of 15 nm AuNP under heat resistance test. (c) The changes of the accumulated flocculation (AF) of 15 nm

1
2
3
4
5
6
7
8
9 AuNP during DTT resistance test. The error was less than 10% based on our absorption
10 measurements. (d) The shifts of SPB (surface plasmon band) of AuNPs during DTT resistance
11 test: MP7M-AuNPs (diamond), BP7M-AuNPs (triangle), DP7M-AuNPs (square) and TP7M-
12 AuNPs (circle). DTT solution: 1.5 M DTT, 0.8 M NaCl and 10 mM NaOH in water.
13
14

15 **Figure 6.** (a) S 2p core line spectra fitted to one or two Voigt doublet(s) (solid line) and
16 superimposed on a polynomial background function (dashed line). Spin-orbit intensity ratio of
17 the S 2p_{1/2} and 2p_{3/2} components was set to 0.5, and the spin-orbit splitting was kept at 1.2 eV.
18 The binding energy of the bound S 2p_{3/2} component was found to be 162 ± 0.1 eV. The spectral
19 intensity of the bound S 2p doublet is indicated by colored shading. (b) Simulated possible
20 conformation of anchoring group of each ligand on the Au surface: MP7M (left up); BP7M
21 (right up); DP7M (left bottom); TP7M (right bottom).
22
23
24
25
26
27

28 **Figure 7.** (a) Modeled possible conformation of DHLA (Left) and TA (right) on the Au surface.
29 (b) DHLA can interact with a pair of gold atoms positioned at two Au threefold hollow sites
30 (Blue filled circles) or two Au bridge sites (Blue open circles), while TA can interact with a pair
31 of atoms positioned at Au threefold hollow site and Au bridge site (Red filled circles).
32
33
34
35
36
37
38
39
40
41
42
43
44
45
46
47
48
49
50
51
52
53
54

1
2
3
4
5
6
7
8
9
10
11
12
13
14
15
16
17
18
19
20
21
22
23
24
25
26
27
28
29
30
31
32
33
34
35
36
37
38
39
40
41
42
43
44
45
46
47
48
49
50
51
52
53
54
55
56
57
58
59
60

1
2
3
4
5
6
7
8
9
10
11
12
13
14
15
16
17
18
19
20
21
22
23
24
25
26
27
28
29
30
31
32
33
34
35
36
37
38
39
40
41
42
43
44
45
46
47
48
49
50
51
52
53
54
55
56
57
58
59
60

References

1. Kim, S. T.; Saha, K.; Kim, C.; Rotello, V. M. The Role of Surface Functionality in Determining Nanoparticle Cytotoxicity. *Acc. Chem. Res.* **2013**, *46* (3), 681-691.
2. Su, S.; Zuo, X. L.; Pan, D.; Pei, H.; Wang, L. H.; Fan, C. H.; Huang, W. Design and Applications of Gold Nanoparticle Conjugates by Exploiting Biomolecule-Gold Nanoparticle Interactions. *Nanoscale* **2013**, *5* (7), 2589-2599.
3. Sapsford, K. E.; Algar, W. R.; Berti, L.; Gemmill, K. B.; Casey, B. J.; Oh, E.; Stewart, M. H.; Medintz, I. L. Functionalizing Nanoparticles with Biological Molecules: Developing Chemistries that Facilitate Nanotechnology. *Chem. Rev.* **2013**, *113* (3), 1904-2074.
4. Saha, K.; Agasti, S. S.; Kim, C.; Li, X. N.; Rotello, V. M. Gold Nanoparticles in Chemical and Biological Sensing. *Chem. Rev.* **2012**, *112* (5), 2739-2779.
5. Alivisatos, P. The Use of Nanocrystals in Biological Detection. *Nat. Biotechnol.* **2004**, *22* (1), 47-52.
6. Daniel, M. C.; Astruc, D. Gold Nanoparticles: Assembly, Supramolecular Chemistry, Quantum-Size-Related Properties, and Applications Toward Biology, Catalysis, and Nanotechnology. *Chem. Rev.* **2004**, *104* (1), 293-346.
7. Katz, E.; Willner, I. Integrated Nanoparticle-Biomolecule Hybrid Systems: Synthesis, Properties, and Applications. *Angew. Chem. Int. Ed. Engl.* **2004**, *43* (45), 6042-6108.
8. Rosi, N. L.; Mirkin, C. A. Nanostructures in Biodiagnostics. *Chem. Rev.* **2005**, *105* (4), 1547-1562.
9. Medintz, I. L.; Uyeda, H. T.; Goldman, E. R.; Mattoussi, H. Quantum Dot Bioconjugates for Imaging, Labelling and Sensing. *Nat. Mater.* **2005**, *4* (6), 435-446.
10. Jennings, T.; Strouse, G. Past, Present, and Future of Gold Nanoparticles. *Adv. Exp. Med. Biol.* **2007**, *620*, 34-47.
11. Sardar, R.; Funston, A. M.; Mulvaney, P.; Murray, R. W. Gold Nanoparticles: Past, Present, and Future. *Langmuir* **2009**, *25* (24), 13840-13851.
12. Nel, A. E.; Madler, L.; Velegol, D.; Xia, T.; Hoek, E. M. V.; Somasundaran, P.; Klaessig, F.; Castranova, V.; Thompson, M. Understanding Biophysicochemical Interactions at the Nano-Bio Interface. *Nat. Mater.* **2009**, *8* (7), 543-557.
13. Otsuka, H.; Nagasaki, Y.; Kataoka, K. PEGylated Nanoparticles for Biological and Pharmaceutical Applications. *Adv Drug Deliver Rev* **2012**, *64*, 246-255.
14. Oh, E.; Fatemi, F. K.; Currie, M.; Delehanty, J. B.; Pons, T.; Fragola, A.; Leveque-Fort, S.; Goswami, R.; Susumu, K.; Huston, A. L.; Medintz, I. L. PEGylated Luminescent Gold Nanoclusters: Synthesis, Characterization, Bioconjugation, and Application to One- and Two-Photon Cellular Imaging. *Part. Part. Syst. Charact.* **2013**, *30* (5), 453-466.
15. Leduc, C.; Si, S.; Gautier, J.; Soto-Ribeiro, M.; Wehrle-Haller, B.; Gautreau, A.; Giannone, G.; Cognet, L.; Lounis, B. A Highly Specific Gold Nanoprobe for Live-Cell Single-Molecule Imaging. *Nano Letters* **2013**, *13* (4), 1489-1494.
16. Hermanson, G. T. *Bioconjugate Techniques*. Academic Press: San Diego, 2008.
17. Love, J. C.; Estroff, L. A.; Kriebel, J. K.; Nuzzo, R. G.; Whitesides, G. M. Self-Assembled Monolayers of Thiolates on Metals as a Form of Nanotechnology. *Chem. Rev.* **2005**, *105* (4), 1103-1169.
18. Pons, T.; Medintz, I. L.; Sapsford, K. E.; Higashiyama, S.; Grimes, A. F.; English, D. S.; Mattoussi, H. On the Quenching of Semiconductor Quantum Dot Photoluminescence by Proximal Gold Nanoparticles. *Nano Lett.* **2007**, *7* (10), 3157-3164.
19. Schultz, F.; Vossmeier, T.; Bastús, N. G.; Weller, H. Effect of the Spacer Structure on the Stability of Gold Nanoparticles Functionalized with Monodentate Thiolated Poly(ethylene glycol) Ligands. *Langmuir* **2013**, *29* (31), 9897-9908.
20. Algar, W. R.; Prasuhan, D. E.; Stewart, M. H.; Jennings, T. L.; Blanco-Canosa, J. B.; Dawson, P. E.; Medintz, I. L. The Controlled Display of Biomolecules on Nanoparticles: A Challenge Suited to Bioorthogonal Chemistry. *Bioconjugate Chem.* **2011**, *22* (5), 825-858.

Formatted: Font: Not Bold

21. Kimling, J.; Maier, M.; Okenve, B.; Kotaidis, V.; Ballot, H.; Plech, A.; Turkevich Method for Gold Nanoparticle Synthesis Revisited. *J. Phys. Chem. B* **2006**, *110* (32), 15700-15707.
22. Weare, W. W.; Reed, S. M.; Warner, M. G.; Hutchison, J. E.; Improved Synthesis of Small (d_{CORE} ~1.5 nm) Phosphine-Stabilized Gold Nanoparticles. *J. Am. Chem. Soc.* **2000**, *122* (51), 12890-12891.
23. Jana, N. R.; Gearheart, L.; Murphy, C. J.; Seeding Growth for Size Control of 5-40 nm Diameter Gold Nanoparticles. *Langmuir* **2001**, *17* (22), 6782-6786.
24. Green, M.; O'Brien, P.; A Simple One Phase Preparation of Organically Capped Gold Nanocrystals. *Chem. Commun.* **2000**, 183-184.
25. Aslam, M.; Fu, L.; Su, M.; Vijayamohan, K.; Dravid, V. P.; Novel One-Step Synthesis of Amine-Stabilized Aqueous Colloidal Gold Nanoparticles. *J. Mater. Chem.* **2004**, *14* (12), 1795-1797.
26. Selvakannan, P. R.; Mandal, S.; Phadtare, S.; Pasricha, R.; Sastry, M.; Capping of Gold Nanoparticles by the Amino Acid Lysine Renders Them Water-Dispersible. *Langmuir* **2003**, *19* (8), 3545-3549.
27. Gandubert, V. J.; Lennox, R. B.; Assessment of 4-(Dimethylamino)pyridine as a Capping Agent for Gold Nanoparticles. *Langmuir* **2005**, *21* (14), 6532-6539.
28. Sharma, J.; Chhabra, R.; Yan, H.; Liu, Y.; A Facile in situ Generation of Dithiocarbamate Ligands for Stable Gold Nanoparticle - Oligonucleotide Conjugates. *Chem. Commun.* **2008**, 2140-2142.
29. Kim, F.; Connor, S.; Song, H.; Kuykendall, T.; Yang, P. D.; Platonic Gold Nanocrystals. *Angew. Chem. Int. Ed.* **2004**, *43* (28), 3673-3677.
30. Lee, Y.; Lee, S. H.; Kim, J. S.; Maruyama, A.; Chen, X. S.; Park, T. G.; Controlled Synthesis of PEI-coated Gold Nanoparticles using Reductive Catechol Chemistry for siRNA Delivery. *J. Control. Rel.* **2011**, *155* (1), 3-10.
31. Hussain, I.; Graham, S.; Wang, Z. X.; Tan, B.; Sherrington, D. C.; Rannard, S. P.; Cooper, A. I.; Brust, M.; Size-Controlled Synthesis of Near-Monodisperse Gold Nanoparticles in the 1-4 nm Range Using Polymeric Stabilizers. *J. Am. Chem. Soc.* **2005**, *127* (47), 16398-16399.
32. You, C. C.; Miranda, O. R.; Gider, B.; Ghosh, P. S.; Kim, I. B.; Erdogan, B.; Krovi, S. A.; Bunz, U. H. F.; Rotello, V. M.; Detection and Identification of Proteins Using Nanoparticle-Fluorescent Polymer 'Chemical Nose' Sensors. *Nat. Nanotechnol.* **2007**, *2* (5), 318-323.
33. Liz-Marzan, L. M.; Giersig, M.; Mulvaney, P.; Synthesis of Nanosized Gold-Silica Core-Shell Particles. *Langmuir* **1996**, *12* (18), 4329-4335.
34. Kairdolf, B. A.; Nie, S. M.; Multidentate-Protected Colloidal Gold Nanocrystals: pH Control of Cooperative Precipitation and Surface Layer Shedding. *J. Am. Chem. Soc.* **2011**, *133* (19), 7268-7271.
35. Brust, M.; Walker, M.; Bethell, D.; Schiffrin, D. J.; Whyman, R.; Synthesis of Thiol-Derivatized Gold Nanoparticles in a Two-Phase Liquid-Liquid System. *J. Chem. Soc., Chem. Commun.* **1994**, (7), 801-802.
36. Yonezawa, T.; Kunitake, T.; Practical Preparation of Anionic Mercapto Ligand-Stabilized Gold Nanoparticles and Their Immobilization. *Colloids Surf. A Physicochemical. Eng. Aspects* **1999**, *149* (1-3), 193-199.
37. Brinas, R. P.; Hu, M. H.; Qian, L. P.; Lyman, E. S.; Hainfeld, J. F.; Gold Nanoparticle Size Controlled by Polymeric Au(I) Thiolate Precursor Size. *J. Am. Chem. Soc.* **2008**, *130* (3), 975-982.
38. Kanaras, A. G.; Kamounah, F. S.; Schaumburg, K.; Kiely, C. J.; Brust, M.; Thioalkylated Tetraethylene Glycol: A New Ligand for Water Soluble Monolayer Protected Gold Clusters. *Chem. Commun.* **2002**, 2294-2295.
39. Wuelfing, W. P.; Gross, S. M.; Miles, D. T.; Murray, R. W.; Nanometer Gold Clusters Protected by Surface-Bound Monolayers of Thiolated Poly(ethylene glycol) Polymer Electrolyte. *J. Am. Chem. Soc.* **1998**, *120* (48), 12696-12697.
40. Oh, E.; Susumu, K.; Blanco-Canosa, J. B.; Medintz, I. L.; Dawson, P. E.; Mattoussi, H.; Preparation of Stable Maleimide-Functionalized Au Nanoparticles and Their Use in Counting Surface Ligands. *Small* **2010**, *6* (12), 1273-1278.
41. Oh, E.; Susumu, K.; Goswami, R.; Mattoussi, H.; One-Phase Synthesis of Water-Soluble Gold Nanoparticles with Control over Size and Surface Functionalities. *Langmuir* **2010**, *26* (10), 7604-7613.

Formatted: Font: Not Bold

1
2
3
4
5
6
7
8
9
10
11
12
13
14
15
16
17
18
19
20
21
22
23
24
25
26
27
28
29
30
31
32
33
34
35
36
37
38
39
40
41
42
43
44
45
46
47
48
49
50
51
52
53
54
55
56
57
58
59
60

42. Susumu, K.; Uyeda, H. T.; Medintz, I. L.; Pons, T.; Delehanty, J. B.; Mattoussi, H.; Enhancing the Stability and Biological Functionalities of Quantum Dots via Compact Multifunctional Ligands. *J. Am. Chem. Soc.* **2007**, *129* (45), 13987-13996.
43. Li, Z.; Jin, R. C.; Mirkin, C. A.; Letsinger, R. L.; Multiple Thiol-Anchor Capped DNA-Gold Nanoparticle Conjugates. *Nucl. Acids. Res.* **2002**, *30* (7), 1558-1562.
44. Levy, R.; Thanh, N. T. K.; Doty, R. C.; Hussain, I.; Nichols, R. J.; Schiffrin, D. J.; Brust, M.; Fernig, D. G.; Rational and Combinatorial Design of Peptide Capping Ligands for Gold Nanoparticles. *J. Am. Chem. Soc.* **2004**, *126* (32), 10076-10084.
45. Tkachenko, A. G.; Xie, H.; Liu, Y. L.; Coleman, D.; Ryan, J.; Glomm, W. R.; Shipton, M. K.; Franzen, S.; Feldheim, D. L.; Cellular Trajectories of Peptide-Modified Gold Particle Complexes: Comparison of Nuclear Localization Signals and Peptide Transduction Domains. *Bioconjugate Chem.* **2004**, *15* (3), 482-490.
46. Oh, E.; Susumu, K.; Jain, V.; Kim, M.; Huston, A.; One-Pot Aqueous Phase Growth of Biocompatible 15-130 nm Gold Nanoparticles Stabilized with Bidentate PEG. *J. Coll. Int. Sci.* **2012**, *376*, 107-111.
47. Susumu, K.; Oh, E.; Delehanty, J. B.; Blanco-Canosa, J. B.; Johnson, B. J.; Jain, V.; Hervey, W. J.; Algar, W. R.; Boeneman, K.; Dawson, P. E.; Medintz, I. L.; Multifunctional Compact Zwitterionic Ligands for Preparing Robust Biocompatible Semiconductor Quantum Dots and Gold Nanoparticles. *J. Am. Chem. Soc.* **2011**, *133* (24), 9480-9496.
48. Hou, W. B.; Dasog, M.; Scott, R. W. J.; Probing the Relative Stability of Thiolate- and Dithiolate-Protected Au Monolayer-Protected Clusters. *Langmuir* **2009**, *25* (22), 12954-12961.
49. Mei, B. C.; Oh, E.; Susumu, K.; Farrell, D.; Mountziaris, T. J.; Mattoussi, H.; Effects of Ligand Coordination Number and Surface Curvature on the Stability of Gold Nanoparticles in Aqueous Solutions. *Langmuir* **2009**, *25* (18), 10604-10611.
50. Mei, B. C.; Susumu, K.; Medintz, I. L.; Delehanty, J. B.; Mountziaris, T. J.; Mattoussi, H.; Modular Poly(ethylene glycol) Ligands for Biocompatible Semiconductor and Gold Nanocrystals with Extended pH and Ionic Stability. *J. Mater. Chem.* **2008**, *18* (41), 4949-4958.
51. Wan, A. S.; Long, J. P.; Kushto, G.; Makinen, A. J.; The Interfacial Chemistry and Energy Level Structure of a Liquid Crystalline Perylene Derivative on Au(111) and Graphite Surfaces. *Chem. Phys. Lett.* **2008**, *463* (1-3), 72-77.
52. Silien, C.; Buck, M.; Goretzki, G.; Lahaye, D.; Champness, N. R.; Weidner, T.; Zharnikov, M.; Self-Assembly of a Pyridine-Terminated Thiol Monolayer on Au(111). *Langmuir* **2009**, *25* (2), 959-967.
53. Wang, J. M.; Wang, W.; Kollman, P. A.; Case, D. A.; Automatic Atom Type and Bond Type Perception in Molecular Mechanical Calculations. *J. Mol. Graph. Model.* **2006**, *25* (2), 247-260.
54. Zheng, J. J.; Yeung, E. S.; Mechanism of Microbial Aggregation During Capillary Electrophoresis. *Anal. Chem.* **2003**, *75* (4), 818-824.
55. Agasti, S. S.; You, C. C.; Arumugam, P.; Rotello, V. M.; Structural Control of the Monolayer Stability of Water-Soluble Gold Nanoparticles. *J. Mater. Chem.* **2008**, *18* (1), 70-73.
56. Dougan, J. A.; Karlsson, C.; Smith, W. E.; Graham, D.; Enhanced Oligonucleotide-Nanoparticle Conjugate Stability Using Thioctic Acid Modified Oligonucleotides. *Nucl. Acids Res.* **2007**, *35* (11), 3668-3675.
57. Meister, A.; Glutathione Metabolism and Its Selective Modification. *J. Biol. Chem.* **1988**, *263* (33), 17205-17208.
58. Petrovykh, D. Y.; Kimura-Suda, H.; Opdahl, A.; Richter, L. J.; Tarlov, M. J.; Whitman, L. J.; Alkanethiols on Platinum: Multicomponent Self-Assembled Monolayers. *Langmuir* **2006**, *22* (6), 2578-2587.
59. Petrovykh, D. Y.; Sullivan, J. M.; Whitman, L. J.; Quantification of Discrete Oxide and Sulfur Layers on Sulfur-Passivated InAs by XPS. *Surf. Interface Anal.* **2005**, *37* (11), 989-997.
60. Widrig, C. A.; Alves, C. A.; Porter, M. D.; Scanning Tunneling Microscopy of Ethanethiolate and n-Octadecanethiolate Monolayers Spontaneously Adsorbed at Gold Surfaces. *J. Am. Chem. Soc.* **1991**, *113* (8), 2805-2810.

Formatted: Font: Not Bold

1
2
3
4
5
6
7
8
9
10
11
12
13
14
15
16
17
18
19
20
21
22
23
24
25
26
27
28
29
30
31
32
33
34
35
36
37
38
39
40
41
42
43
44
45
46
47
48
49
50
51
52
53
54
55
56
57
58
59
60

61. Vance, A. L.; Willey, T. M.; Nelson, A. J.; van Buuren, T.; Bostedt, C.; Terminello, L. J.; Fox, G. A.; Engelhard, M.; Baer, D.; XAS and XPS Characterization of Monolayers Derived from a Dithiol and Structurally Related Disulfide-Containing Polyamides. *Langmuir* **2002**, *18* (21), 8123-8128.
62. Jang, Y. H.; Goddard, W. A.; Electron Transport through Cyclic Disulfide Molecular Junctions with Two Different Adsorption States at the Contact: A Density Functional Theory Study. *J. Phys. Chem. C* **2008**, *112* (23), 8715-8720.
63. Fenter, P.; Eberhardt, A.; Eisenberger, P.; Self-Assembly of n-Alkyl Thiols as Disulfides on Au(111). *Science* **1994**, *266* (5188), 1216-1218.

Formatted: Font: Not Bold

Formatted: Font: Not Bold

Formatted: Font: Not Bold

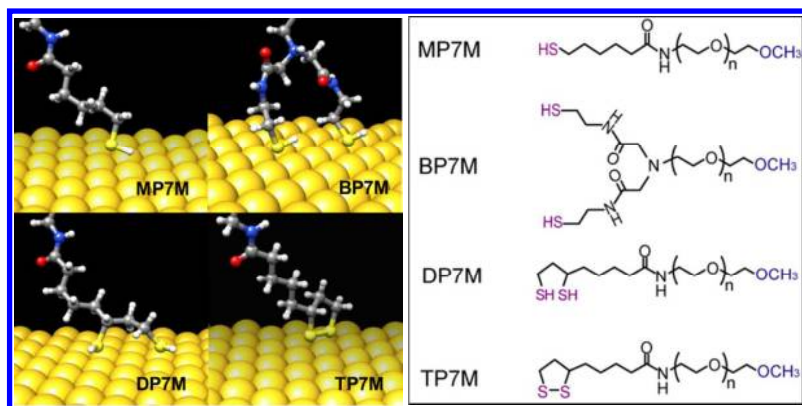
Table of contents entry

Colloidal Stability of Gold Nanoparticles Coated with Multithiol-Poly(ethylene glycol) Ligands: Importance of Structural Constraints of the Sulfur Anchoring Groups

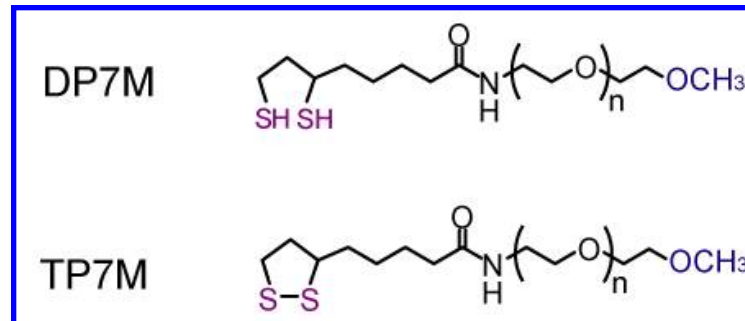
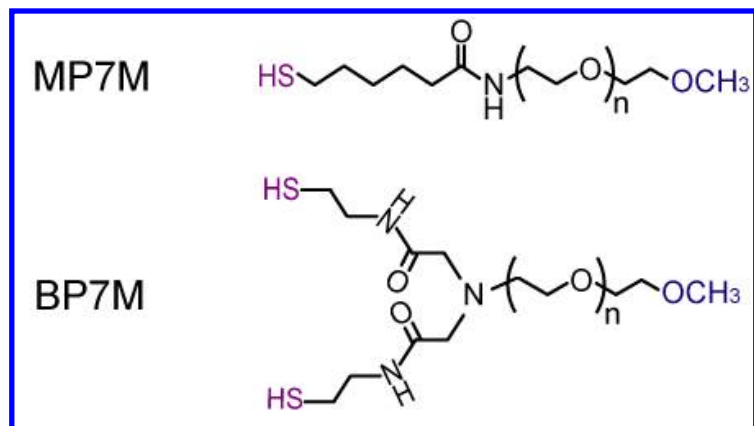
TOC Keywords: Disulfide, Bidentate, Monothiol, Constrained dithiol, DTT

Eunkeu Oh, Kimihiro Susumu, Antti J. Mäkinen, Jeffrey R. Deschamps, Alan L. Huston and Igor L. Medintz

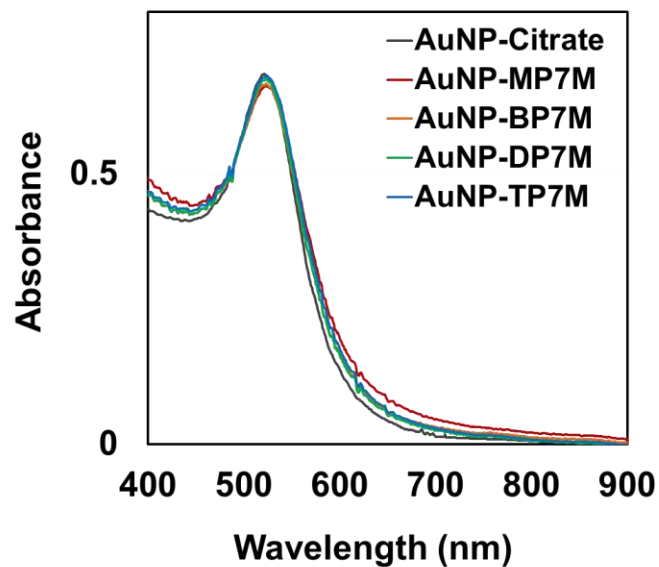
TOC figure



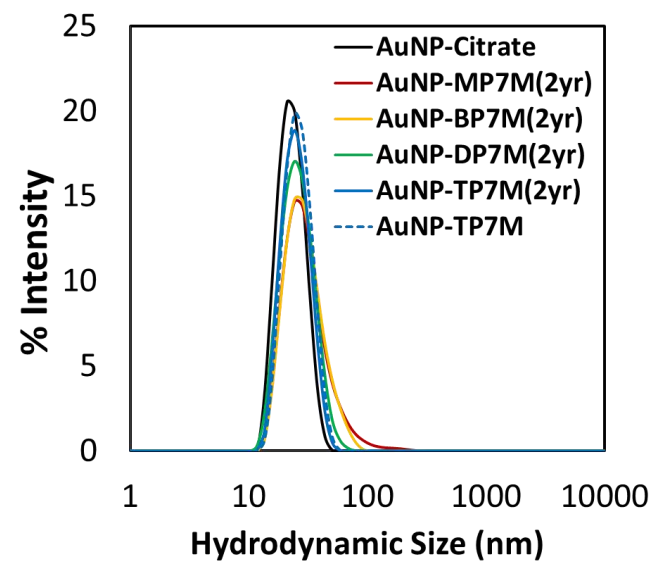
(a)



(b)



(c)



1

2

3 (a)

4

5

6

7

8

9

10

11

12

13

14

15

16

17

18

19

20

21

22

23

24

25

26

27

28

29

30

31

32

33

34

35

36

37

38

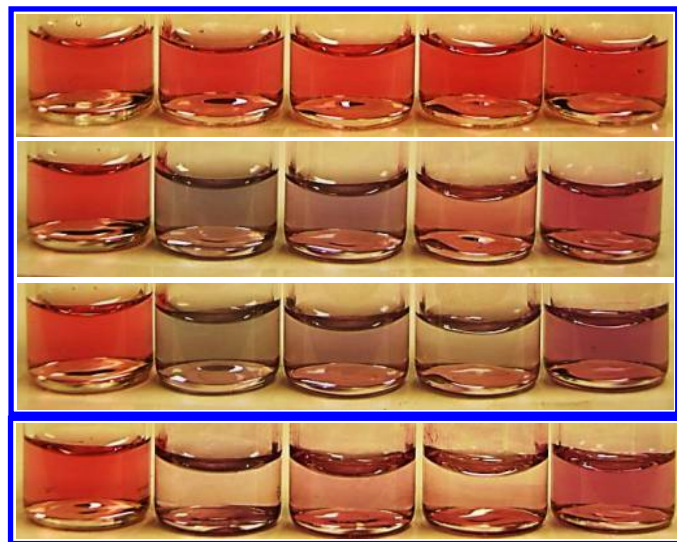
39

40

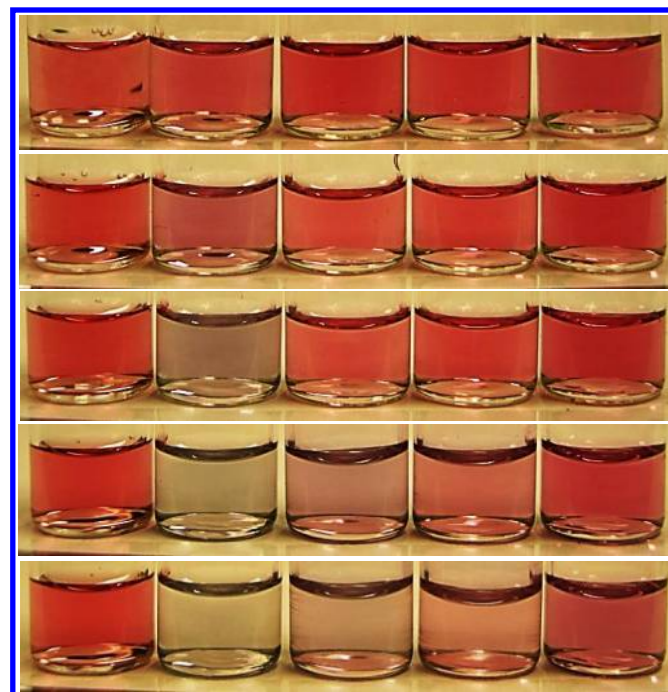
41

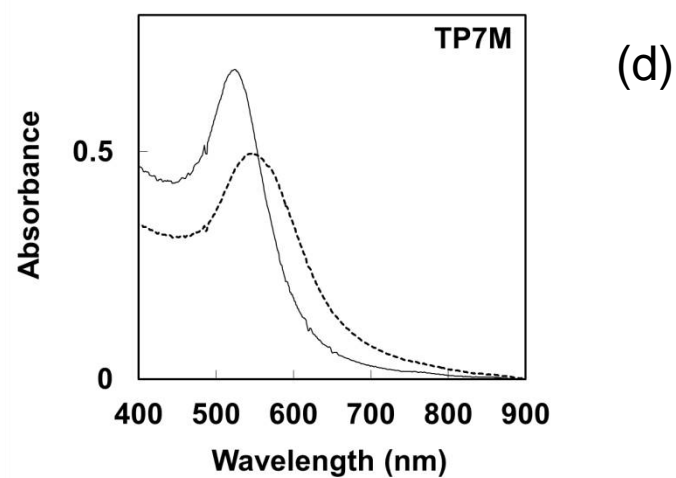
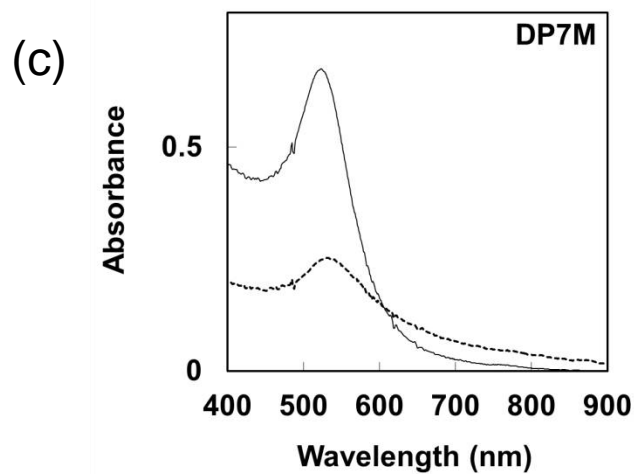
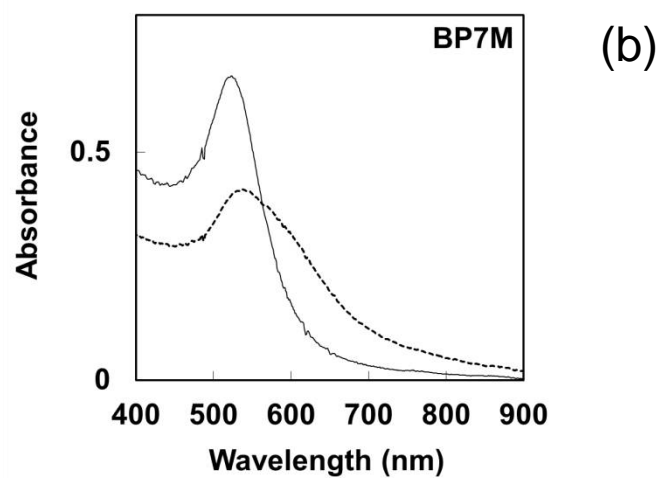
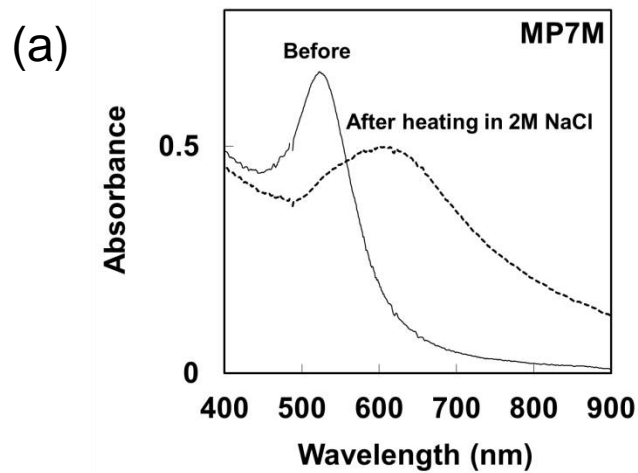
42

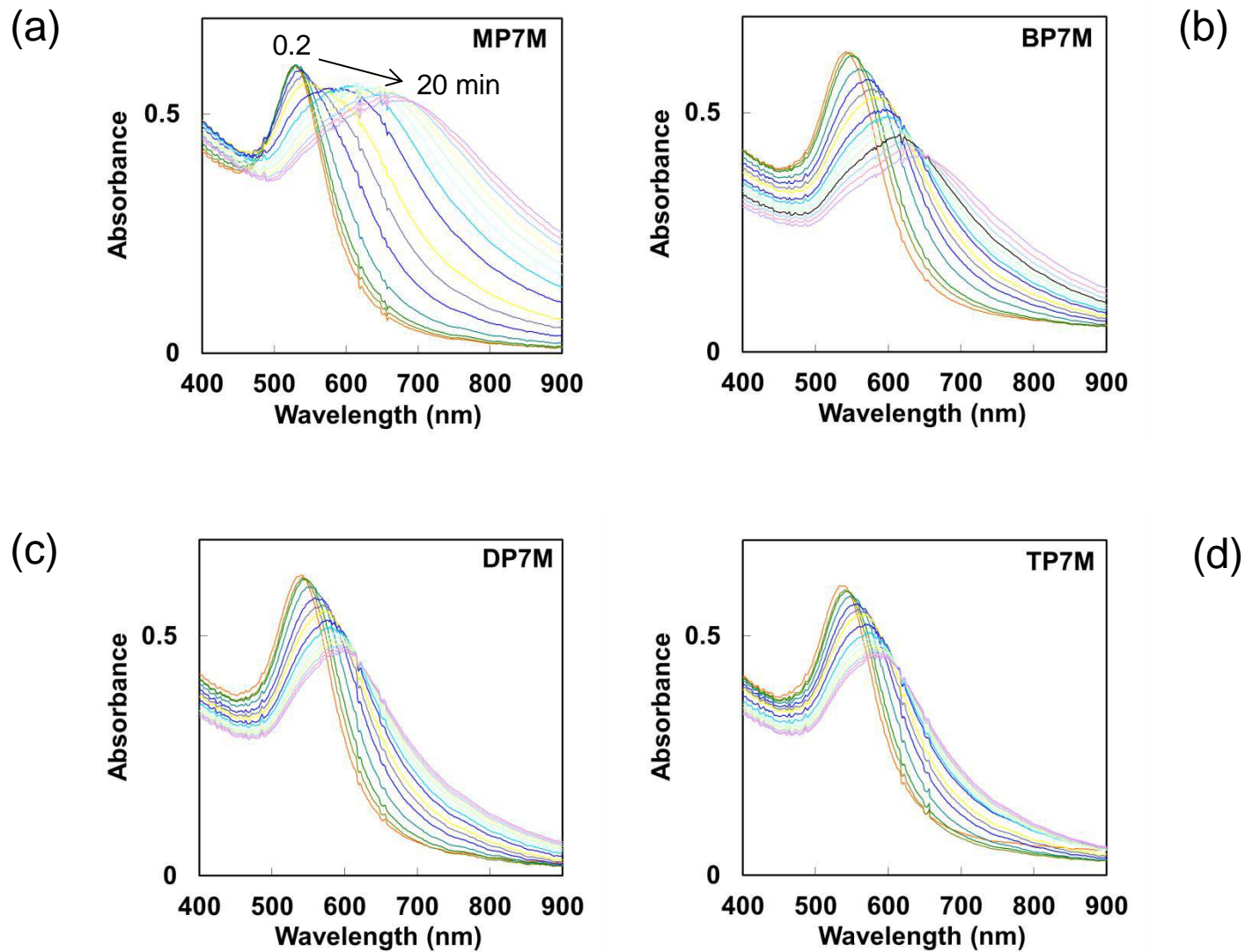
43

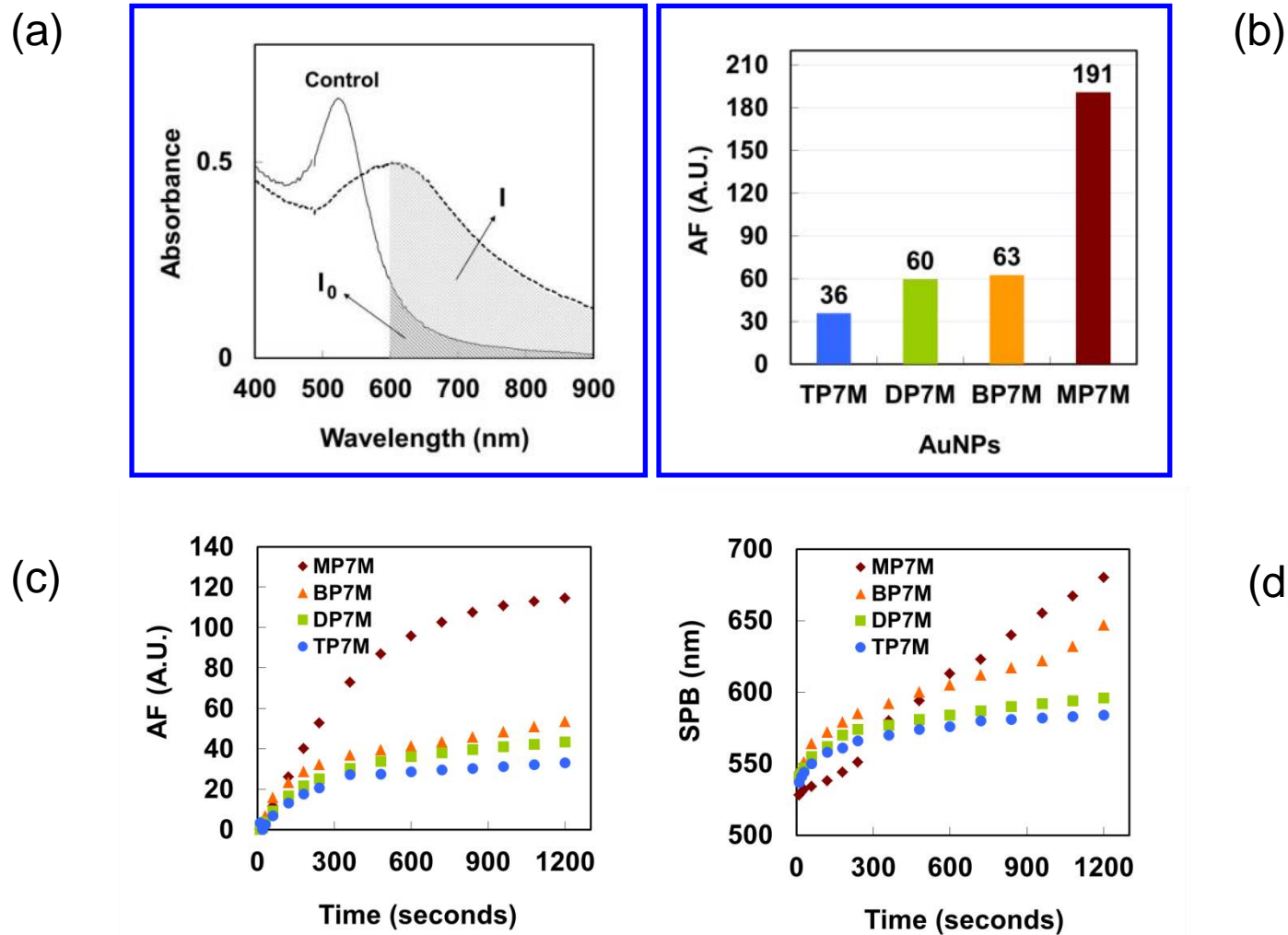
2 M NaCl at 100°C**0 min****5 min****15 min****15 min at 100°C
+ 24 hr at RT****Cont. MP7M BP7M DP7M TP7M**

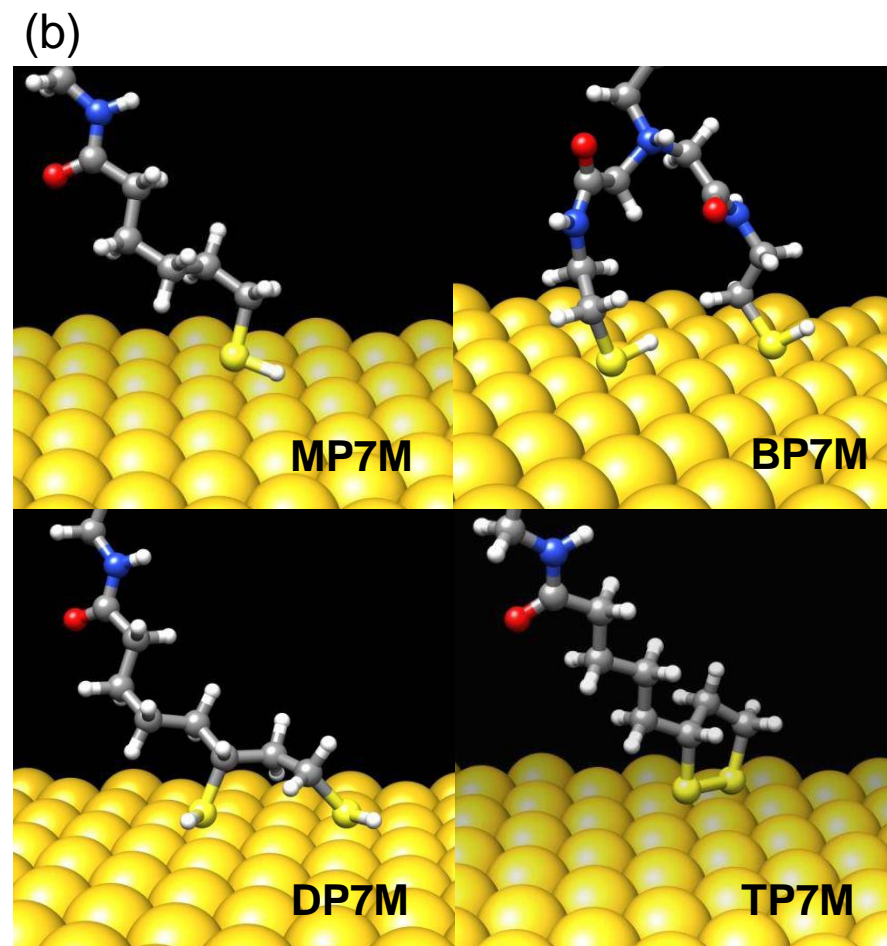
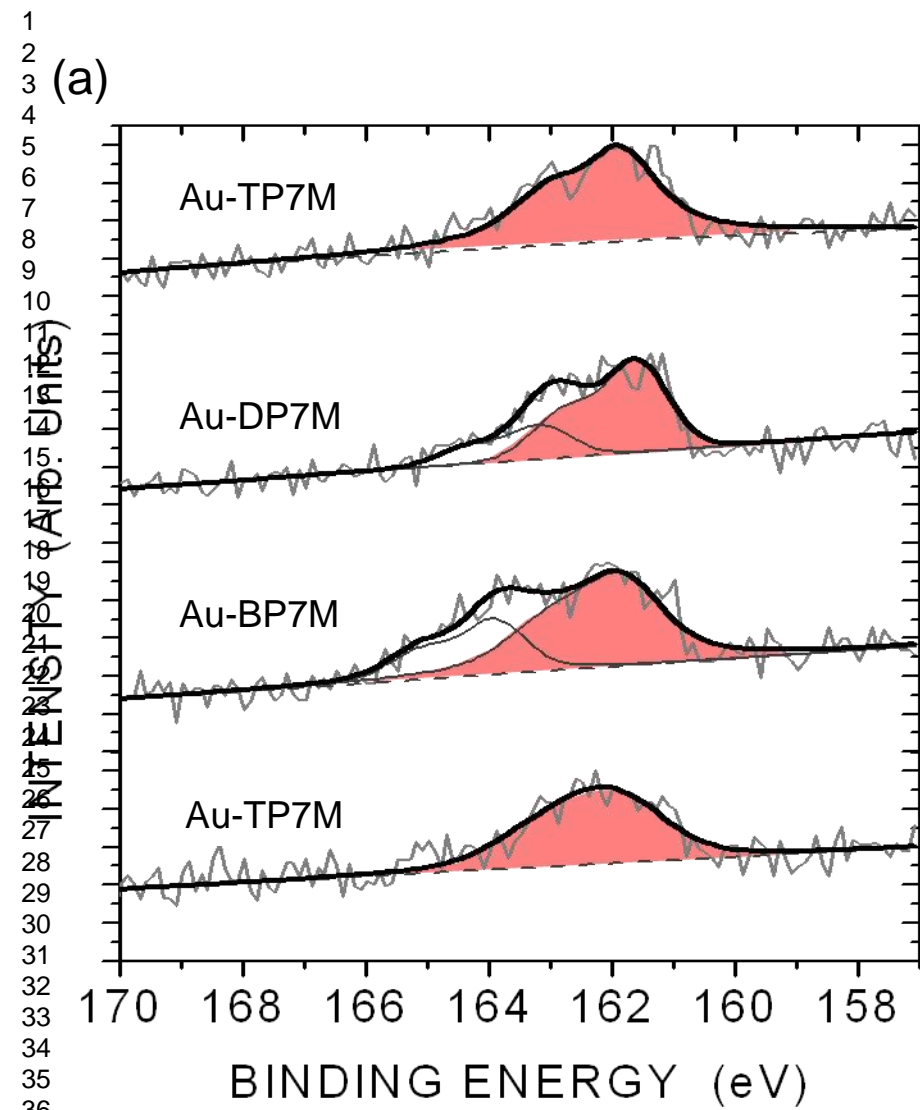
(b)

1.5 M DTT, 0.8 M NaCl, 10 mM NaOH**1 min****4 min****20 min****60 min****90 min****Cont. MP7M BP7M DP7M TP7M**



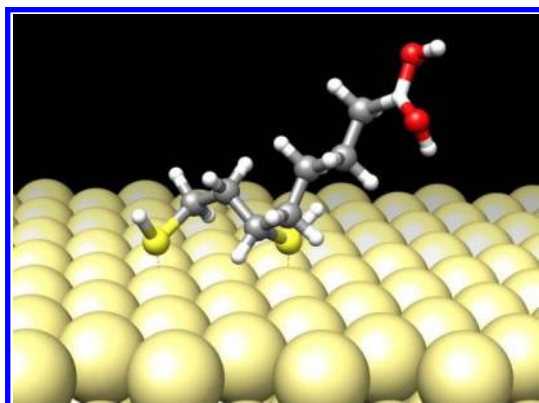




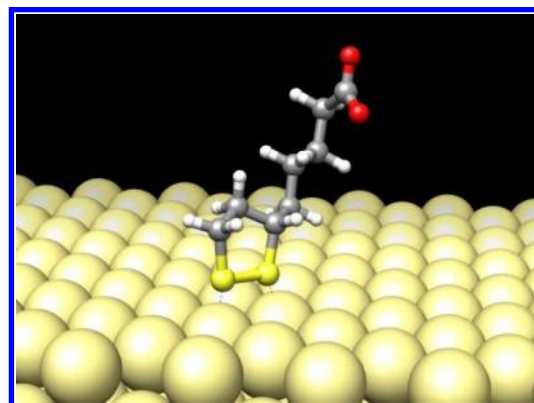


(a)

DHHLA



TA



(b)

